Available online at www.sciencedirect.com
SCIENCE DIRECT®
Journal of Molecular Spectroscopy 218 (2003) 85–94
Journal of MOLECULAR SPECTROSCOPY
www.elsevier.com/locate/jms

Studies of the mid- and far-infrared laser magnetic resonance spectra of the CD radical: information on vibrationally excited levels

Martin Wienkoop,[a] Wolfgang Urban,[a,1] Jonathan P. Towle,[b,2] John M. Brown,[b,*] and Kenneth M. Evenson[c,3]

[a] *Institut für Angewandte Physik, Universität Bonn, Wegelerstrasse 8, D53115 Bonn, Germany*
[b] *The Physical and Theoretical Chemistry Laboratory, South Parks Road, Oxford OX1 3QZ, UK*
[c] *Time and Frequency Division, NIST, 325 Broadway, Boulder, CO 80303, USA*

Received 27 August 2002

Abstract

Two separate studies of the CD radical in vibrationally excited levels of its $X^2\Pi$ ground state have been made by the technique of laser magnetic resonance. The first of these studies was in the far-infrared; rotational transitions of CD in the $v = 1$ and 2 levels have been detected. The second study was carried out in the mid-infrared using a carbon monoxide laser magnetic resonance spectrometer. In these experiments, transitions in the (1,0), (2,1), and (3,2) bands have been detected. All the available data on CD in its $X^2\Pi$ state have been used to determine an improved set of molecular parameters for the CD radical. In addition to the above data sets, previous far-infrared laser magnetic resonance on the CD radical in the $v = 0$ level and FTIR observations of the (1,0) and (2,1) bands have been included. The principal molecular parameters determined are: $\nu_0 = 2032.03360\ (18)\,\mathrm{cm}^{-1}$, $\omega_e x_e = 34.72785\ (58)\,\mathrm{cm}^{-1}$, $B_0 = 7.7018632\ (14)\,\mathrm{cm}^{-1}$, $\alpha_B = -\alpha_e = -0.212239\ (11)\,\mathrm{cm}^{-1}$, where the figures given in parentheses are one standard deviation from the least squares fit. A small but significant dependence of the orbital contribution to the magnetic dipole moment on the vibrational quantum number is detected. This may reflect the mixing between the $X^2\Pi$ and $a^4\Sigma^-$ states of CD.

1. Introduction

The CH radical is a leading player on the stage of physical chemistry. It is an enthusiastic participant in many combustion processes [1] and is widespread in astronomical sources such as the interstellar medium [2–4]. As befits such an important species, it has been the subject of extensive spectroscopic study over the years. Less attention has been paid to its deuterated isotopomer, CD, although the deficit is being made good by recent work. The present paper can be regarded as a further contribution to our knowledge of CD.

The first spectroscopic information on CD came from its electronic spectrum which has been studied successively by Shindei [5], Gerö [6] and by Herzberg and Johns [7]. Pure rotational and spin–rotational transitions in CD in its $X^2\Pi$ state were observed at far-infrared wavelengths by Brown and Evenson [8] using the technique of laser magnetic resonance (LMR). This provided the first really precise measurement of several molecular parameters, including the rotational constant, the spin–orbit coupling constant, lambda-doubling parameters and the deuteron hyperfine parameters. More recently, Morino et al. [9] have recorded the infrared spectrum in emission with a Fourier transform interferometer. They observed lines in the (1,0) and (2,1) bands of CD.

Two types of spectroscopic observation on CD are reported in the present paper. First, in an extension of the work of Brown and Evenson [8], far-infrared LMR spectra of CD in the excited vibrational levels $v = 1$ and 2 have been recorded. Second, the mid-infrared

* Corresponding author. Fax: 44-1865-275410.
E-mail address: jmb@physchem.ox.ac.uk (J.M. Brown).
[1] Present address: Adelheidstrasse 7, D 61462 Königstein, Germany.
[2] Present address: 38 Hawthorne Drive, #F303, Bedford, NH 03110, USA.
[3] To the great loss of the whole scientific community, Ken Evenson died on 29 January 2002.

0022-2852/03/$ - see front matter © 2003 Elsevier Science (USA). All rights reserved.
doi:10.1016/S0022-2852(02)00064-4

spectrum has been recorded again but this time more accurately by the technique of CO LMR. Resonances in the (1,0), (2,1), and (3,2) vibrational bands have been identified and measured. These new observations have been combined with those from earlier studies of CD in the $X^2\Pi$ state [8,9] to produce an improved set of vibration–rotation parameters for this molecule.

2. Experimental details

The far-infrared LMR experiments were performed at the Boulder laboratories of NIST as in the earlier work on CD [8]; the spectrometer has been described in detail elsewhere [10]. The CD radicals were produced in the spectrometer sample volume by the reaction of fluorine atoms with deuterated methane in a flow system, the fluorine atoms being generated by passing a mixture of 10% F_2 in helium through a microwave discharge. The total pressure in the sample volume was about 0.33 mbar (33 Pa) which permitted Lamb dips to be observed on most of the strong lines. The optimum reaction conditions to produce vibrationally excited CD were essentially the same as those required to produce CD in the $v = 0$ level, an indication of the marked exothermicity of the reactions involved. The magnetic field was modulated at a frequency of 14 kHz and the signal detected with a lock-in amplifier at the same frequency. The resonances were consequently displayed as the first derivative of an absorption profile. The magnet of the LMR system was controlled by a rotating-coil magnetometer which provided a direct readout of the flux densities. The system was calibrated periodically up to 1.8 T with a proton NMR gaussmeter; the absolute uncertainty was 10^{-5} T below 0.1 T and the fractional uncertainty was 10^{-4} above 0.1 T.

The mid-infrared LMR experiments were conducted at the Institut für Angewandte Physik at the University of Bonn in Germany. The apparatus was in the Faraday rotation configuration and has been described in detail previously, for example [11]. The carbon monoxide laser was liquid-nitrogen cooled and of the flowing gas type. Initially, the CD radicals were produced in these experiments in an electric discharge through a mixture of CD_4, D_2, and helium. The D_2 gas was included because it suppressed the formation of a graphite film on the cell wall; if present, this film tended to break away and so cause large noise spikes in the signal channel. In the course of this work, it was discovered that CD signals which were almost as strong (~80%) could be obtained by running the discharge through a mixture of CH_4, D_2, and helium. This provided a much cheaper method of producing the signals; CD_4 was only used when a very weak signal was expected. The optimum pressures in the gas discharge were 3.3 mbar (330 Pa) of He, 0.5 mbar (50 Pa) of D_2, and 0.1 mbar (10 Pa) of CH_4. The signal intensities also showed a dependence on the discharge current. Lines in the fundamental band reached a maximum level at a current of 75 mA. Lines in the (2,1) and (3,2) bands on the other hand were still increasing when the current was at its maximum value of 150 mA. The magnetic field in these experiments was provided by a super-conducting solenoid with a maximum flux density of 3.2 T. A region at the center of the magnet of length 30 cm was modulated at 8.6 kHz. The signal was pre-amplified and passed to a lock-in amplifier tuned to the modulation frequency. The signals therefore appear as the first derivative of a dispersion profile.

3. Results and analysis

3.1. Far-infrared observations

The far-infrared observations on CD in excited vibrational levels are summarised in Table 1. One rotational transition was observed in the $v = 1$ level and three in $v = 2$. An example from the 171.8 μm spectrum is shown in Fig. 1. The transition involved is $N = 4 \leftarrow 3$, $+ \leftarrow -$ of CD in the $v = 2$ level. The deuteron triplet hyperfine structure ($I = 1$) can be clearly seen as a series of Lamb dips on each of the main resonances. The detailed measurements for the three laser lines used are given in Table 2. The assignments were made with the help of a computer program which predicted all possible resonances for a given laser frequency, together with their lines strengths and tuning rates. This information constitutes the Zeeman pattern which can be used to make the assignments even when the molecular parameters employed are not quite accurate. The molecular parameters were estimated from the corresponding values for CH [12,13] using appropriate isotopic scaling factors and also from the work of Morino et al. [9]. The resultant assignments are also given in Table 2. The quantum numbers used to describe the molecular states are N, the parity, the spin component identification number, M_J and M_I (the nuclear spin de-coupled description is the appropriate one for experiments performed in a magnetic field although some weak transitions which violate the selection rule $\Delta M_I = 0$ were observed, see Table 2). The electron spin identification number counts the states with given values of parity, N, M_J, and M_I in order of increasing energy. It is used in preference to the quantum number J because the latter ceases to be good, even in quite modest magnetic fields. This occurs because the spin–rotation splittings in CD are very small. As explained by Brown and Evenson [8], CD conforms almost perfectly to Hund's case (b) coupling because A is almost exactly equal to $4B$. An estimate of the experimental uncertainty of each observation is given in Table 2; this is dominated by the accuracy of the far-infrared laser frequencies which are re-settable to $\sqrt{2} \times 5 \times 10^{-7}\, \nu_L$.

Table 1
FIR laser lines used to record LMR spectra of the CD radical in vibrationally excited levels

CO_2 pump	Gain medium	Wavelength (μm)	Frequency (MHz)	CD transitions observed			
				v	N	J	F_i[a]
10R(20)	CH_2F_2	166.6	1 799 139.3	1	$4 \leftarrow 3$	$3\frac{1}{2} \leftarrow 2\frac{1}{2}$	$F_2 \leftarrow F_2$
9R(8)	$^{13}CH_3OH$	171.8	1 745 439.0	2	$4 \leftarrow 3$	$3\frac{1}{2} \leftarrow 2\frac{1}{2}$	$F_2 \leftarrow F_2$
						$4\frac{1}{2} \leftarrow 3\frac{1}{2}$	$F_1 \leftarrow F_1$
9R(10)	CH_3OH	232.9	1 286 999.5	2	$3 \leftarrow 2$	$3\frac{1}{2} \leftarrow 2\frac{1}{2}$	$F_2 \leftarrow F_2$
					$2 \leftarrow 1$	$1\frac{1}{2} \leftarrow \frac{1}{2}$	$F_2 \leftarrow F_2$

[a] F_i labels the spin components in order of increasing energy for a given J.

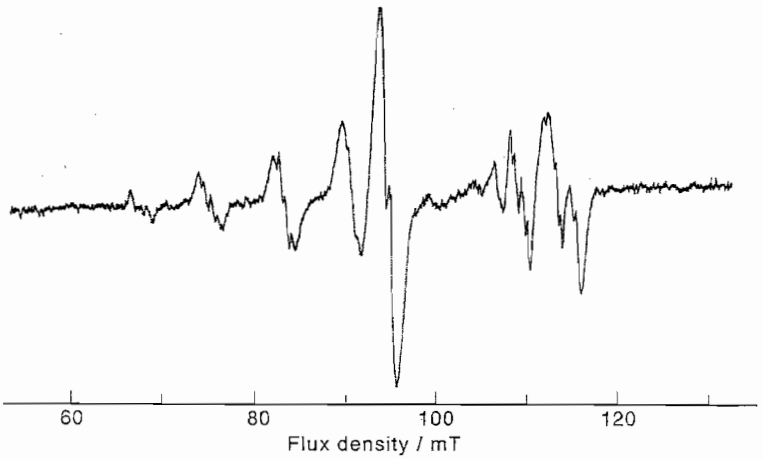

Fig. 1. Part of the far-infrared LMR spectrum of the CD radical in excited vibrational levels of the $X^2\Pi$ state. The spectrum is recorded with the 171.8 μm laser line in perpendicular polarization ($\Delta M_J = \pm 1$). The rotational transition involved is $N = 4 \leftarrow 3$, $+ \leftarrow -$ of CD in the $v = 2$ level. The deuteron triplet hyperfine structure can be seen on most of the main resonances as Lamb dips.

3.2. Mid-infrared observations

The mid-infrared observations were made with a carbon monoxide laser, using lines between 2050 and 1850 cm^{-1}. Transitions in three vibration–rotation bands were observed. The first few lines in the Q- and P-branches were seen in the fundamental band, R- and Q-lines were seen in the (2,1) band and P-, Q-, and R-lines were seen in the (3,2) band. The details of the observations are given in Tables 3–5. The assignments, which are also given in these tables, were made with the help of the same predictive computer program, using the parameters from the work of Morino et al. [9]. An example of the mid-infrared LMR observations is shown in Fig. 2. The resonances are associated with the P-branch transition, $N = 1 \leftarrow 2$, $F_1 \leftarrow F_1$ ($J = 1\frac{1}{2} \leftarrow 2\frac{1}{2}$) in the fundamental band at 2000.09 cm^{-1}. The lambda-type doubling can be clearly seen. Because of the greater Doppler linewidth in the mid-infrared, the deuteron hyperfine structure is not resolved in any of these spectra. The uncertainty of a single, non-overlapped line is estimated to be 30 MHz or 0.001 cm^{-1}.

3.3. Determination of molecular parameters

An improved set of molecular parameters was determined by fitting a model Hamiltonian to all the available data on CD in its $X^2\Pi$ state by least-squares methods. The data set is comprised of four parts:

(i) the far-infrared LMR data reported by Brown and Evenson [8] on the spin–rotation transitions of CD in its $v = 0$ level (198 data points),

(ii) the FTIR measurements of Morino et al. [9] on the (1,0) and (2,1) transitions of CD in zero magnetic field (103 data points),

(iii) the far-infrared LMR data on spin–rotation transitions of CD in the $v = 1$ and 2 levels reported in this work (67 data points, see Table 2) and

(iv) the mid-infrared LMR data on the (1,0), (2,1), and (3,2) bands of CD also reported in this paper (111 data points, see Tables 3–5).

The data were weighted inversely as the square of the estimated experimental uncertainty in the least-squares fit. Morino et al. [9] did not give an estimate of their experimental uncertainty. We have assigned a value of 60 MHz or 0.002 cm^{-1} to this quantity.

Table 2
Observations in the far-infrared LMR spectrum of the CD radical in vibrationally excited states

v	$N' \leftarrow N''$	Parity	$M_J' \leftarrow M_J''$	M_I	Eigenstate id. #[a]	B_0 (mT)	$\nu_L - \nu_{calc}$ (MHz)	$\partial\nu/\partial B_0$ (MHz/mT)	Uncert. (MHz)
166.6 μm spectrum ν_L = 1 799 139.3 MHz									
1	4 ← 3	+ ← −	$-3\frac{1}{2} \leftarrow -3\frac{1}{2}$	$-1 \leftarrow -1$	2 ← 2	477.36	−0.60	21.77	2.0
		+ ← −		$0 \leftarrow 0$	2 ← 2	477.81	−0.84	21.76	2.0
		+ ← −		$1 \leftarrow 1$	2 ← 2	478.27	−1.29	21.76	2.0
		+ ← −	$-2\frac{1}{2} \leftarrow -2\frac{1}{2}$	[b]	2 ← 2	974.70	−0.48	4.36	1.27
		− ← +	$-2\frac{1}{2} \leftarrow -2\frac{1}{2}$	[b]	2 ← 2	1675.08	0.75	3.58	1.27
		− ← +	$-1\frac{1}{2} \leftarrow -2\frac{1}{2}$	[b]	2 ← 2	1054.18	−1.44	5.59	1.27
		+ ← −	$-\frac{1}{2} \leftarrow -1\frac{1}{2}$	[b]	2 ← 2	1089.61	−0.63	3.67	1.27
171.8 μm spectrum ν_L = 1 745 439.0 MHz									
2	4 ← 3	+ ← −	$-2\frac{1}{2} \leftarrow -2\frac{1}{2}$	$-1 \leftarrow -1$	1 ← 1	82.47	−0.31	−8.10	1.23
		+ ← −		$0 \leftarrow 0$	1 ← 1	83.19	−0.14	−8.09	1.23
		+ ← −		$1\frac{1}{2} \leftarrow 1\frac{1}{2}$	1 ← 1	83.90	−0.16	−8.09	1.23
		+ ← −	$-1\frac{1}{2} \leftarrow -1\frac{1}{2}$	$-1 \leftarrow -1$	1 ← 1	89.64	−0.05	−5.78	1.23
		+ ← −		$0 \leftarrow 0$	1 ← 1	90.24	−0.82	−5.78	1.23
		+ ← −		$1 \leftarrow 1$	1 ← 1	90.82	0.21	−5.77	1.23
		+ ← −	$\frac{1}{2} \leftarrow \frac{1}{2}$	[b]	1 ← 1	99.90	0.45	−4.01	1.23
		+ ← −	$-3\frac{1}{2} \leftarrow -3\frac{1}{2}$	$-1 \leftarrow -1$	2 ← 2	133.4	0.11	22.73	2.0
		+ ← −		$0 \leftarrow 0$	2 ← 2	133.8	1.48	22.72	2.0
		+ ← −		$1 \leftarrow 1$	2 ← 2	134.3	0.60	22.70	2.0
		+ ← −	$-2\frac{1}{2} \leftarrow -2\frac{1}{2}$	$-1 \leftarrow -1$	2 ← 2	209.26	0.10	7.36	1.23
		+ ← −		$0 \leftarrow 0$	2 ← 2	209.60	−0.20	7.37	1.23
		+ ← −		$1 \leftarrow 1$	2 ← 2	209.89	−0.12	7.38	1.23
		− ← +	$-3\frac{1}{2} \leftarrow -3\frac{1}{2}$	$-1 \leftarrow -1$	2 ← 2	298.4	1.49	22.60	2.0
		− ← +		$0 \leftarrow 0$	2 ← 2	298.8	−0.43	22.60	2.0
		− ← +		$1 \leftarrow 1$	2 ← 2	299.3	−4.61	22.60	2.0
		+ ← −	$-1\frac{1}{2} \leftarrow -1\frac{1}{2}$	[b]	2 ← 2	375.49	−0.23	29.47	1.23
		− ← +	$-2\frac{1}{2} \leftarrow -2\frac{1}{2}$	[b]	2 ← 2	827.44	−1.16	3.62	1.23
		+ ← −	$-\frac{1}{2} \leftarrow -\frac{1}{2}$	[b]	2 ← 2	901.12	−0.48	1.05	1.23
		− ← +	$-1\frac{1}{2} \leftarrow -1\frac{1}{2}$	[b]	2 ← 2	1582.2	−0.66	2.00	2.0
		+ ← −	$-1\frac{1}{2} \leftarrow -2\frac{1}{2}$	$-1 \leftarrow -1$	1 ← 1	66.8	−0.22	−8.14	2.0
		+ ← −		$0 \leftarrow 0$	1 ← 1	67.7	0.48	−8.16	2.0
		+ ← −		$1 \leftarrow 1$	1 ← 1	68.6	1.09	−8.18	2.0
		+ ← −	$-\frac{1}{2} \leftarrow -1\frac{1}{2}$	$-1 \leftarrow -1$	1 ← 1	74.2	−0.31	−5.95	2.0
		+ ← −		$0 \leftarrow 0$	1 ← 1	75.0	−0.16	−5.94	2.0
		+ ← −		$1 \leftarrow 1$	1 ← 1	75.8	−0.02	−5.94	2.0
2	4 ← 3	+ ← −	$\frac{1}{2} \leftarrow -\frac{1}{2}$	$-1 \leftarrow -1$	1 ← 1	82.5	−0.34	−4.46	2.0
		+ ← −		$0 \leftarrow 0$	1 ← 1	83.2	−0.08	−4.45	2.0
		+ ← −		$1 \leftarrow 1$	1 ← 1	83.9	0.02	−4.44	2.0
		+ ← −	$1\frac{1}{2} \leftarrow \frac{1}{2}$	$-1 \leftarrow -1$	1 ← 1	90.1	−0.01	−3.61	2.0
		+ ← −		$0 \leftarrow 0$	1 ← 1	90.6	0.20	−3.60	2.0
		+ ← −		$1 \leftarrow 1$	1 ← 1	91.1	0.30	−3.59	2.0
		+ ← −	$3\frac{1}{2} \leftarrow 2\frac{1}{2}$	[b]	1 ← 1	94.6	0.47	−3.36	2.0
		+ ← −	$-\frac{1}{2} \leftarrow -1\frac{1}{2}$	[b]	2 ← 2	249.5	−0.52	5.17	2.0
		+ ← −	$-3\frac{1}{2} \leftarrow -2\frac{1}{2}$	$-1 \leftarrow -1$	2 ← 2	323.8	0.30	3.60	1.23
		+ ← −		$0 \leftarrow 0$	2 ← 2	324.5	0.27	3.60	1.23
		+ ← −		$1 \leftarrow 1$	2 ← 2	325.15	0.41	3.60	1.23
		+ ← −	$\frac{1}{2} \leftarrow -\frac{1}{2}$	[b]	2 ← 2	444.1	−0.56	2.39	2.0
		− ← +	$-1\frac{1}{2} \leftarrow -2\frac{1}{2}$	[b]	2 ← 2	536.4	−1.70	5.379	2.0
		− ← +	$-\frac{1}{2} \leftarrow -1\frac{1}{2}$	[b]	2 ← 2	916.42	−2.58	3.23	1.27
		+ ← −	$-2\frac{1}{2} \leftarrow -1\frac{1}{2}$	[b]	2 ← 2	945.06	−0.44	0.88	1.27
		− ← +	$-3\frac{1}{2} \leftarrow -2\frac{1}{2}$	[b]	2 ← 2	1658.71	1.90	1.95	1.27
232.9 μm spectrum ν_L = 1 286 999.5 MHz									
2	2 ← 1	− ← +	$-\frac{1}{2} \leftarrow -\frac{1}{2}$	$-1 \leftarrow -1$	1 ← 1	682.18	−0.16	−11.65	0.91
		− ← +		$0 \leftarrow 0$	1 ← 1	682.45	0.40	−11.65	0.91
		− ← +		$1 \leftarrow 1$	1 ← 1	682.65	0.22	−11.65	0.91
		+ ← −	$-\frac{1}{2} \leftarrow -\frac{1}{2}$	[b]	1 ← 1	687.94	−2.02	−12.01	0.91
		+ ← −	$-\frac{1}{2} \leftarrow \frac{1}{2}$	$1 \leftarrow 0$	1 ← 1	689.49	1.44	−12.01	0.91
		− ← +	$\frac{1}{2} \leftarrow \frac{1}{2}$	$-1 \leftarrow -1$	1 ← 1	982.85	−0.65	−8.08	0.91
		− ← +		$0 \leftarrow 0$	1 ← 1	983.42	0.26	−8.08	0.91

Table 2 (*continued*)

	$N' \leftarrow N''$	Parity	$M_J' \leftarrow M_J''$	M_I	Eigenstate id. #[a]	B_0 (mT)	$\nu_L - \nu_{calc}$ (MHz)	$\partial\nu/\partial B_0$ (MHz/mT)	Uncert. (MHz)
2	$2 \leftarrow 1$	$- \leftarrow +$		$1 \leftarrow 1$	$1 \leftarrow 1$	983.91	0.49	−8.08	0.91
		$+ \leftarrow -$	$\frac{1}{2} \leftarrow \frac{1}{2}$	$1 \leftarrow 1$	$1 \leftarrow 1$	992.22	0.56	−8.24	2.0
		$+ \leftarrow -$		$0 \leftarrow 0$	$1 \leftarrow 1$	993.25[c]	0.88	−8.24	2.82
		$+ \leftarrow -$		$-1 \leftarrow -1$	$1 \leftarrow 1$	993.25[c]	1.48	−8.24	2.82
	$3 \leftarrow 2$	$+ \leftarrow -$	$-1\frac{1}{2} \leftarrow -1\frac{1}{2}$	$-1 \leftarrow -1$	$1 \leftarrow 2$	1223.23	0.27	−17.16	0.91
		$+ \leftarrow -$		$0 \leftarrow 0$	$1 \leftarrow 2$	1223.76	0.98	−17.16	0.91
		$+ \leftarrow -$		$1 \leftarrow 1$	$1 \leftarrow 2$	1224.31	1.69	−17.15	0.91
	$2 \leftarrow 1$	$- \leftarrow +$	$-1\frac{1}{2} \leftarrow -\frac{1}{2}$	[b]	$1 \leftarrow 1$	596.23	−0.40	−13.17	0.91
		$+ \leftarrow -$	$-1\frac{1}{2} \leftarrow -\frac{1}{2}$	$-1 \leftarrow -1$	$2 \leftarrow 1$	603.02	−0.16	−13.75	0.91
		$+ \leftarrow -$	$-1\frac{1}{2} \leftarrow \frac{1}{2}$	$1 \leftarrow 0$	$2 \leftarrow 1$	604.13	0.98	−13.74	0.91
		$- \leftarrow +$	$-\frac{1}{2} \leftarrow \frac{1}{2}$	[b]	$2 \leftarrow 1$	680.51	−0.68	−11.68	0.91

[a] Identification number labels the eigenstate with the correct values for M_J and M_I in order of increasing energy for a given value for N.
[b] Deuteron hyperfine structure not resolved.
[c] Two hyperfine components assigned to the same resonance.

Table 3
Observations in the mid-infrared LMR spectrum of the CD radical: lines in the fundamental (1,0) band

$N' - N''$	Parity	$M_J \leftarrow M_J''$	Eigenstate id. #[a]	B_0 (mT)	$\nu_L \nu_{calc}$ (MHz)	$\partial\nu/\partial B_0$ (MHz/mT)	Uncert. (MHz)
$P(11)_{3,2}$: 2046.95900 cm^{-1} or 61 366.28696 GHz							
$1 \leftarrow 1$	$+ \leftarrow -$	$1\frac{1}{2} \leftarrow \frac{1}{2}$	$1 \leftarrow 1$	2065.3	16	13.12	30
	$- \leftarrow +$	$1\frac{1}{2} \leftarrow \frac{1}{2}$	$1 \leftarrow 1$	2035.3	43	13.13	30
$P(8)_{4,3}$: 2033.14256 cm^{-1} or 60 952.08049 GHz							
$2 \leftarrow 2$	$+ \leftarrow -$	$\frac{1}{2} \leftarrow -\frac{1}{2}$	$2 \leftarrow 2$	2346.5	157	24.78	60
	$+ \leftarrow -$	$1\frac{1}{2} \leftarrow \frac{1}{2}$	$2 \leftarrow 2$	2346.5	108	23.23	60
	$- \leftarrow +$	$\frac{1}{2} \leftarrow -\frac{1}{2}$	$2 \leftarrow 2$	2431.5	164	24.96	60
	$- \leftarrow +$	$1\frac{1}{2} \leftarrow \frac{1}{2}$	$2 \leftarrow 2$	2431.5	45	23.43	60
	$+ \leftarrow -$	$-\frac{1}{2} \leftarrow -1\frac{1}{2}$	$2 \leftarrow 2$	2696.4	136	23.14	30
	$- \leftarrow +$	$-\frac{1}{2} \leftarrow -1\frac{1}{2}$	$2 \leftarrow 2$	2794.8	163	23.29	30
	$+ \leftarrow -$	$2\frac{1}{2} \leftarrow 1\frac{1}{2}$	$1 \leftarrow 1$	2846.6	124	16.71	60
	$- \leftarrow +$	$2\frac{1}{2} \leftarrow 1\frac{1}{2}$	$1 \leftarrow 1$	2939.4	116	16.89	60
$P(15)_{3,2}$: 2030.15878 cm^{-1} or 60 862.62920 GHz							
$3 \leftarrow 3$	$+ \leftarrow -$	$\frac{1}{2} \leftarrow -\frac{1}{2}$	$2 \leftarrow 2$	527.2	23	17.69	30
	$+ \leftarrow -$	$-\frac{1}{2} \leftarrow \frac{1}{2}$	$2 \leftarrow 2$	622.6	20	16.59	30
	$+ \leftarrow -$	$-1\frac{1}{2} \leftarrow -\frac{1}{2}$	$2 \leftarrow 2$	812.5	22	16.87	30
$2 \leftarrow 2$	$- \leftarrow +$	$-2\frac{1}{2} \leftarrow -1\frac{1}{2}$	$1 \leftarrow 1$	1322.6	−24	−14.23	30
	$+ \leftarrow -$	$-2\frac{1}{2} \leftarrow -1\frac{1}{2}$	$1 \leftarrow 1$	1400.2	−45	−14.24	30
	$- \leftarrow +$	$-1\frac{1}{2} \leftarrow -\frac{1}{2}$	$2 \leftarrow 2$	2544.5	−22	−0.53	30
	$+ \leftarrow -$	$-1\frac{1}{2} \leftarrow -\frac{1}{2}$	$2 \leftarrow 2$	2901.0	−22	−5.12	30
$P(9)_{4,3}$: 2029.12784 cm^{-1} or 60 831.72224 GHz							
$3 \leftarrow 3$	$+ \leftarrow -$	$-3\frac{1}{2} \leftarrow -2\frac{1}{2}$	$1 \leftarrow 1$	676.0	−28	−14.28	30
	$- \leftarrow +$	$-3\frac{1}{2} \leftarrow -2\frac{1}{2}$	$1 \leftarrow 1$	979.9	−40	−17.20	30
$4 \leftarrow 4$	$+ \leftarrow -$	$\frac{1}{2} \leftarrow 1\frac{1}{2}$	$2 \leftarrow 2$	1106.2	51	24.05	[b]
	$+ \leftarrow -$	$\frac{1}{2} \leftarrow -\frac{1}{2}$	$2 \leftarrow 2$	1128.4	23	25.47	60
	$+ \leftarrow -$	$1\frac{1}{2} \leftarrow 2\frac{1}{2}$	$2 \leftarrow 2$	1044.1	100	23.82	[b]
	$+ \leftarrow -$	$1\frac{1}{2} \leftarrow \frac{1}{2}$	$2 \leftarrow 2$	1055.5	15	25.40	60
	$+ \leftarrow -$	$-\frac{1}{2} \leftarrow \frac{1}{2}$	$2 \leftarrow 2$	1181.0	78	24.09	30
	$+ \leftarrow -$	$-1\frac{1}{2} \leftarrow -\frac{1}{2}$	$2 \leftarrow 2$	1278.2	70	23.98	30
$2 \leftarrow 2$	$+ \leftarrow -$	$1\frac{1}{2} \leftarrow 2\frac{1}{2}$	$1 \leftarrow 1$	1691.4	−65	−17.12	60
$4 \leftarrow 4$	$- \leftarrow +$	$-1\frac{1}{2} \leftarrow -\frac{1}{2}$	$2 \leftarrow 2$	1765.2	94	24.77	[b]
$2 \leftarrow 2$	$- \leftarrow +$	$-1\frac{1}{2} \leftarrow -\frac{1}{2}$	$1 \leftarrow 1$	1779.4	−116	−21.41	60
	$- \leftarrow +$	$\frac{1}{2} \leftarrow -\frac{1}{2}$	$1 \leftarrow 1$	2346.2	−85	−16.46	30

Table 3 (*continued*)

$N' \leftarrow N''$	Parity	$M_J \leftarrow M_J''$	Eigenstate id. #[a]	B_0 (mT)	$\nu_L \nu_{calc}$ (MHz)	$\partial\nu/\partial B_0$ (MHz/mT)	Uncert. (MHz)
	$-\leftarrow+$	$1\frac{1}{2} \leftarrow \frac{1}{2}$	$1 \leftarrow 1$	2395.9	−68	−14.43	30
	$+\leftarrow-$	$\frac{1}{2} \leftarrow -\frac{1}{2}$	$1 \leftarrow 1$	2471.1	−76	−16.62	30
	$+\leftarrow-$	$1\frac{1}{2} \leftarrow \frac{1}{2}$	$1 \leftarrow 1$	2526.1	−76	−14.62	30
	$-\leftarrow+$	$-\frac{1}{2} \leftarrow -1\frac{1}{2}$	$1 \leftarrow 1$	2822.9	−88	−15.59	30
$2 \leftarrow 2$	$+\leftarrow-$	$-\frac{1}{2} \leftarrow -1\frac{1}{2}$	$1 \leftarrow 1$	2969.7	−99	−15.65	30
	$-\leftarrow+$	$-2\frac{1}{2} \leftarrow -1\frac{1}{2}$	$1 \leftarrow 1$	3153.5	−114	−18.38	30
$3 \leftarrow 3$	$+\leftarrow-$	$-2\frac{1}{2} \leftarrow -1\frac{1}{2}$	$2 \leftarrow 2$	2683.4	71	−2.35	30
$P(12)_{4,3}$: 2016.88220 cm^{-1} or 60 464.60423 GHz							
$1 \leftarrow 1$	$-\leftarrow+$	$\frac{1}{2} \leftarrow 1\frac{1}{2}$	$1 \leftarrow 1$	12.0	11	−13.6	30
	$+\leftarrow-$	$-\frac{1}{2} \leftarrow -1\frac{1}{2}$	$1 \leftarrow 1$	22.7	41	13.55	30
	$+\leftarrow-$	$\frac{1}{2} \leftarrow -\frac{1}{2}$	$1 \leftarrow 1$	72.0	23	4.51	30
$P(16)_{4,3}$: 2000.09007 cm^{-1} or 59 961.1919 GHz							
$1 \leftarrow 2$	$-\leftarrow+$	$-1\frac{1}{2} \leftarrow -\frac{1}{2}$	$1 \leftarrow 1$	1368.4	−47	−19.67	30
	$+\leftarrow-$	$-1\frac{1}{2} \leftarrow -\frac{1}{2}$	$1 \leftarrow 1$	1432.5	−64	−19.76	30
	$-\leftarrow+$	$-\frac{1}{2} \leftarrow \frac{1}{2}$	$2 \leftarrow 2$	1698.0	−49	−15.57	30
	$+\leftarrow-$	$-\frac{1}{2} \leftarrow \frac{1}{2}$	$2 \leftarrow 2$	1778.6	−61	−15.63	30
	$-\leftarrow+$	$\frac{1}{2} \leftarrow 1\frac{1}{2}$	$2 \leftarrow 2$	2509.7	−55	−10.22	30
	$+\leftarrow-$	$\frac{1}{2} \leftarrow 1\frac{1}{2}$	$2 \leftarrow 2$	2629.5	−49	−10.27	30
$P(10)_{5,4}$: 1999.15216 cm^{-1} or 59 933.0740 GHz							
$1 \leftarrow 2$	$+\leftarrow-$	$-1\frac{1}{2} \leftarrow -\frac{1}{2}$	$1 \leftarrow 1$	2750.1	−80	−22.40	30
	$-\leftarrow+$	$-1\frac{1}{2} \leftarrow -\frac{1}{2}$	$1 \leftarrow 1$	2687.7	−90	−22.37	30
$P(13)_{5,4}$: 1986.91149 cm^{-1} or 59 566.1078 GHz							
$2 \leftarrow 3$	$-\leftarrow+$	$-\frac{1}{2} \leftarrow \frac{1}{2}$	$2 \leftarrow 2$	3057.1	126	20.50	30
	$+\leftarrow-$	$-\frac{1}{2} \leftarrow \frac{1}{2}$	$2 \leftarrow 2$	3183.6	166	20.65	30
$P(14)_{5,4}$: 1982.76489 cm^{-1} or 59 441.79601 GHz							
$2 \leftarrow 3$	$+\leftarrow-$	$-1\frac{1}{2} \leftarrow -2\frac{1}{2}$	$1 \leftarrow 1$	2512.2	−34	−22.28	30
	$-\leftarrow+$	$-1\frac{1}{2} \leftarrow -2\frac{1}{2}$	$1 \leftarrow 1$	2616.1	−33	−22.18	30
	$+\leftarrow-$	$1\frac{1}{2} \leftarrow 2\frac{1}{2}$	$1 \leftarrow 1$	2287.8	16	−17.37	30
	$-\leftarrow+$	$1\frac{1}{2} \leftarrow 2\frac{1}{2}$	$1 \leftarrow 1$	2337.1	−57	−17.31	30
$P(9)_{7,6}$: 1951.45547 cm^{-1} or 58 503.1632 GHz							
$4 \leftarrow 5$	$+\leftarrow-$	$\frac{1}{2} \leftarrow -\frac{1}{2}$	$2 \leftarrow 2$	442.0	47	23.82	30
	$+\leftarrow-$	$-1\frac{1}{2} \leftarrow -2\frac{1}{2}$	$2 \leftarrow 2$	593.7	62	22.37	30
	$-\leftarrow+$	$-\frac{1}{2} \leftarrow -1\frac{1}{2}$	$2 \leftarrow 2$	165.4	73	6.20	30
	$-\leftarrow+$	$-1\frac{1}{2} \leftarrow -2\frac{1}{2}$	$2 \leftarrow 2$	316.8	36	10.13	30
	$-\leftarrow+$	$-2\frac{1}{2} \leftarrow -3\frac{1}{2}$	$2 \leftarrow 2$	498.9	31	14.75	30
	$-\leftarrow+$	$-3\frac{1}{2} \leftarrow -4\frac{1}{2}$	$2 \leftarrow 2$	713.5	23	19.26	60

[a] Identification number labels the eigenstate with the correct value for M_J in order of increasing energy for a given value for N.
[b] Measurement given zero weight in the least-squares fit.

The effective Hamiltonian was cast in the N^2 form as described by Brown et al. [14] with the Zeeman terms as described in [15]. This is the same Hamiltonian as was used in the earlier work on the far-infrared LMR spectrum of CD [8] and also on its FTIR spectrum [9]. The eigenstates were identified in terms of Hund's case (b) quantum numbers as described above. The basis set was truncated at states with $\Delta N = \pm 2$ which reproduced the exact calculations to within a few kHz for the highest field resonances. The parameter A_D was constrained to zero in the fit as a result of which the parameters A and γ are effective parameters [16]. The vibrational dependence of each parameter was described in the general form [17]

$$P_v = P_e + \alpha_P(v + 1/2) + \beta_P(v + 1/2)^2 + \ldots. \quad (1)$$

Thus, for the vibrational dependence of the rotational constant,

$$\alpha_B = -\alpha_e \text{ and } \beta_B = \gamma_e, \quad (2)$$

in terms of the more traditional notation [18].

The results of the least-squares fit are given in Tables 2–5 and the parameters determined in the process are given in Table 6 in both MHz and cm^{-1} units.

Table 4
Observations in the mid-infrared LMR spectrum of the CD radical: lines in the (2,1) hot band

$N' \leftarrow N''$	Parity	$M_J' \leftarrow M_J''$	Eigenstate id. #[a]	B_0 (mT)	$\nu_L - \nu_{calc}$ (MHz)	$\partial\nu/\partial B_0$ (MHz/mT)	Uncert. (MHz)
$P(8)_{5,4}$: 2007.14522 cm^{-1} or 60 172.7000 GHz							
$3 \leftarrow 2$	$- \leftarrow +$	$-2\frac{1}{2} \leftarrow -1\frac{1}{2}$	$2 \leftarrow 2$	1228.5	62	20.35	30
	$+ \leftarrow -$	$-2\frac{1}{2} \leftarrow -1\frac{1}{2}$	$2 \leftarrow 2$	1324.2	60	20.33	30
$P(5)_{6,5}$: 1992.84936 cm^{-1} or 59 744.1209 GHz							
$2 \leftarrow 1$	$+ \leftarrow -$	$\frac{1}{2} \leftarrow -\frac{1}{2}$	$2 \leftarrow 2$	1382.2	58	17.32	30
	$- \leftarrow +$	$\frac{1}{2} \leftarrow -\frac{1}{2}$	$2 \leftarrow 2$	1461.9	37	17.31	30
	$+ \leftarrow -$	$1\frac{1}{2} \leftarrow \frac{1}{2}$	$2 \leftarrow 2$	2105.6	37	11.11	30
	$- \leftarrow +$	$1\frac{1}{2} \leftarrow \frac{1}{2}$	$2 \leftarrow 2$	2219.3	32	11.12	30
$P(12)_{5,4}$: 1991.02499 cm^{-1} or 59 689.4277 GHz							
$2 \leftarrow 1$	$- \leftarrow +$	$-1\frac{1}{2} \leftarrow -\frac{1}{2}$	$1 \leftarrow 1$	2423.8	63	−11.73	30
	$+ \leftarrow -$	$-1\frac{1}{2} \leftarrow -\frac{1}{2}$	$1 \leftarrow 1$	2572.0	−55	−11.76	60
$P(15)_{5,4}$: 1978.58535 cm^{-1} or 59 316.4967 GHz							
$1 \leftarrow 1$	$- \leftarrow +$	$1\frac{1}{2} \leftarrow \frac{1}{2}$	$1 \leftarrow 1$	2312.4	44	12.73	30
	$+ \leftarrow -$	$1\frac{1}{2} \leftarrow \frac{1}{2}$	$1 \leftarrow 1$	2336.9	24	1.280	30
$P(9)_{6,5}$: 1977.27417 cm^{-1} or 59 277.1884 GHz							
$1 \leftarrow 1$	$+ \leftarrow -$	$-1\frac{1}{2} \leftarrow -\frac{1}{2}$	$1 \leftarrow 1$	706.0	−47	−12.96	30
	$- \leftarrow +$	$-1\frac{1}{2} \leftarrow -\frac{1}{2}$	$1 \leftarrow 1$	745.4	−47	−12.89	30
	$+ \leftarrow -$	$-\frac{1}{2} \leftarrow \frac{1}{2}$	$2 \leftarrow 2$	2417.5	−25	−3.28	30
	$- \leftarrow +$	$-\frac{1}{2} \leftarrow \frac{1}{2}$	$2 \leftarrow 2$	2543.5	−46	−3.23	30
$P(6)_{7,6}$: 1963.08282 cm^{-1} or 58 851.7423 GHz							
$1 \leftarrow 1$	$- \leftarrow +$	$1\frac{1}{2} \leftarrow \frac{1}{2}$	$1 \leftarrow 1$	113.1	32	8.41	60
	$- \leftarrow +$	$\frac{1}{2} \leftarrow -\frac{1}{2}$	$2 \leftarrow 2$	113.1	−0	8.72	60
	$- \leftarrow +$	$-\frac{1}{2} \leftarrow -1\frac{1}{2}$	$2 \leftarrow 2$	113.1	−33	9.03	60
	$+ \leftarrow -$	$\frac{1}{2} \leftarrow 1\frac{1}{2}$	$2 \leftarrow 2$	47.7	−25	−8.90	60
	$+ \leftarrow -$	$-\frac{1}{2} \leftarrow \frac{1}{2}$	$2 \rightarrow 2$	47.7	−34	−8.72	60
	$+ \leftarrow -$	$-1\frac{1}{2} \leftarrow -\frac{1}{2}$	$1 \leftarrow 1$	47.7	−43	−8.54	60
$2 \leftarrow 2$	$- \leftarrow +$	$-\frac{1}{2} \leftarrow -1\frac{1}{2}$	$2 \leftarrow 2$	3046.8	18	5.85	30
	$+ \leftarrow -$	$1\frac{1}{2} \leftarrow \frac{1}{2}$	$1 \leftarrow 1$	2360.5	23	6.01	30
	$- \leftarrow +$	$1\frac{1}{2} \leftarrow \frac{1}{2}$	$1 \leftarrow 1$	2754.5	−62	6.34	60
	$+ \leftarrow -$	$-\frac{1}{2} \leftarrow -1\frac{1}{2}$	$2 \leftarrow 2$	2714.5	77	6.15	60
	$- \leftarrow +$	$\frac{1}{2} \leftarrow 1\frac{1}{2}$	$2 \leftarrow 2$	602.1	26	11.94	30
	$- \leftarrow +$	$-\frac{1}{2} \leftarrow \frac{1}{2}$	$2 \leftarrow 2$	672.4	12	13.011	30
	$+ \leftarrow -$	$-1\frac{1}{2} \leftarrow -\frac{1}{2}$	$2 \leftarrow 2$	722.0	−26	10.69	30
$P(10)_{7,6}$: 1947.51216 cm^{-1} or 58 384.9458 GHz							
$1 \leftarrow 1$	$+ \leftarrow -$	$\frac{1}{2} \leftarrow 1\frac{1}{2}$	$1 \leftarrow 1$	2725.6	−58	−13.07	30
	$- \leftarrow +$	$\frac{1}{2} \leftarrow 1\frac{1}{2}$	$1 \leftarrow 1$	2744.4	−57	−13.14	30

[a] Identification number labels the eigenstate with the correct value for M_J in order of increasing energy for a given value for N.

Some of the smaller parameters ($\omega_e z_e$, H, β_D, g_l', and g_r^e) have been constrained to values estimated from other sources [19,15]. The values adopted are given in the Table. The electron spin g-factor is constrained to a value of 2.0020, which corresponds to a relativistic correction of 1.5×10^{-4}. The standard deviation of the fit of 479 data points relative to experimental uncertainties is 1.358, a figure which can be regarded as reasonably satisfactory (a value of 1.0 is expected if the model is adequate and the weighting factors have been chosen correctly). The details of the fits of the $v = 0$ far-infrared LMR spectra and the FTIR data are not reproduced here. They are essentially the same as reported earlier [8,9].

4. Discussion

Observations of the LMR spectra of the CD radical in vibrationally excited levels have been made at far- and mid-infrared wavelengths. In a fit of all the available data on the CD radical in its $X^2\Pi$ state, an improved set of molecular parameters has been obtained, as given in Table 6. The zero-point values of the parameters are essentially the same as those given earlier by Brown and Evenson [8,20] because their measurements for the $v = 0$ level have been included in the fit. The only apparent discrepancy is in the value for g_L which differs significantly from the earlier value of 1.000661 (76). This arises because the orbital Zeeman term in the Hamiltonian has

Table 5
Observations in the mid-infrared LMR spectrum of the CD radical: lines in the (3,2) hot band

$N' \leftarrow N''$	Parity	$M_J' \leftarrow M_J''$	Eigenstate id. #[a]	B_0 (mT)	$\nu_L \nu_{calc}$ (MHz)	$\partial\nu/\partial B_0$ (MHz/mT)	Uncert. (MHz)
$P(6)_{8,7}$: 1937.23337 cm^{-1} or 58 076.7955 GHz							
$3 \leftarrow 2$	$+ \leftarrow -$	$-1\frac{1}{2} \leftarrow -\frac{1}{2}$	$1 \leftarrow 1$	290.7	−37	−5.78	60
	$+ \leftarrow -$	$-2\frac{1}{2} \leftarrow -1\frac{1}{2}$	$1 \leftarrow 1$	290.0	−63	−5.24	60
	$+ \leftarrow -$	$-2\frac{1}{2} \leftarrow -1\frac{1}{2}$	$2 \leftarrow 2$	387.7	−38	8.37	30
	$+ \leftarrow -$	$2\frac{1}{2} \leftarrow 1\frac{1}{2}$	$1 \leftarrow 1$	513.2	−90	−5.54	30
	$- \leftarrow +$	$2\frac{1}{2} \leftarrow 1\frac{1}{2}$	$1 \leftarrow 1$	871.9	−44	−4.52	30
$P(13)_{8,7}$: 1909.87748 cm^{-1} or 57 256.6864 GHz							
$1 \leftarrow 1$	$- \leftarrow +$	$1\frac{1}{2} \leftarrow \frac{1}{2}$	$1 \leftarrow 1$	302.6	6	12.50	30
	$+ \leftarrow -$	$1\frac{1}{2} \leftarrow \frac{1}{2}$	$1 \leftarrow 1$	334.1	−8	12.57	30
$P(10)_{9,8}$: 1896.16939 cm^{-1} or 56 845.7281 GHz							
$1 \leftarrow 1$	$+ \leftarrow -$	$1\frac{1}{2} \leftarrow \frac{1}{2}$	$1 \leftarrow 1$	2987.3	23	6.90	60
	$+ \leftarrow -$	$\frac{1}{2} \leftarrow -\frac{1}{2}$	$2 \leftarrow 2$	2678.8	68	8.37	60
	$- \leftarrow +$	$\frac{1}{2} \leftarrow -\frac{1}{2}$	$2 \leftarrow 2$	2858.0	48	8.35	60
	$- \leftarrow +$	$-\frac{1}{2} \leftarrow -1\frac{1}{2}$	$2 \leftarrow 2$	2585.1	42	9.91	30
$2 \leftarrow 2$	$+ \leftarrow -$	$\frac{1}{2} \leftarrow 1\frac{1}{2}$	$2 \leftarrow 2$	2310.9	247	15.70	60
	$+ \leftarrow -$	$-\frac{1}{2} \leftarrow \frac{1}{2}$	$2 \leftarrow 2$	2092.9	91	17.93	30
	$+ \leftarrow -$	$-1\frac{1}{2} \leftarrow -\frac{1}{2}$	$2 \leftarrow 2$	2317.7	−23	16.62	60
	$- \leftarrow +$	$-\frac{1}{2} \leftarrow \frac{1}{2}$	$2 \leftarrow 2$	2207.5	56	18.03	60
$P(7)_{10,9}$: 1882.02699 cm^{-1} or 56 421.7497 GHz							
$1 \leftarrow 1$	$- \leftarrow +$	$-\frac{1}{2} \leftarrow -1\frac{1}{2}$	$1 \leftarrow 1$	1889.2	69	12.97	30
	$+ \leftarrow -$	$-\frac{1}{2} \leftarrow -1\frac{1}{2}$	$1 \leftarrow 1$	1929.8	63	12.90	30
$P(14)_{9,8}$: 1880.34277 cm^{-1} or 56 371.2582 GHz							
$1 \leftarrow 1$	$+ \leftarrow -$	$\frac{1}{2} \leftarrow 1\frac{1}{2}$	$1 \leftarrow 1$	1987.2	−73	−12.76	30
	$- \leftarrow +$	$\frac{1}{2} \leftarrow 1\frac{1}{2}$	$1 \leftarrow 1$	2011.7	−4	−12.83	30
$P(15)_{10,9}$: 1850.92272 cm^{-1} or 55 489.2672 GHz							
$2 \leftarrow 3$	$+ \leftarrow -$	$-1\frac{1}{2} \leftarrow -2\frac{1}{2}$	$2 \leftarrow 2$	1958.9	−32	−4.14	30
	$- \leftarrow +$	$-1\frac{1}{2} \leftarrow -2\frac{1}{2}$	$2 \leftarrow 2$	2527.5	−51	−4.00	30
	$+ \leftarrow -$	$-\frac{1}{2} \leftarrow \frac{1}{2}$	$2 \leftarrow 2$	1426.3	−45	−4.52	60
	$- \leftarrow +$	$-\frac{1}{2} \leftarrow \frac{1}{2}$	$2 \leftarrow 2$	1800.0	−1	−4.47	60

[a] Identification number labels the eigenstate with the correct value for M_J in order of increasing energy for a given value for N.

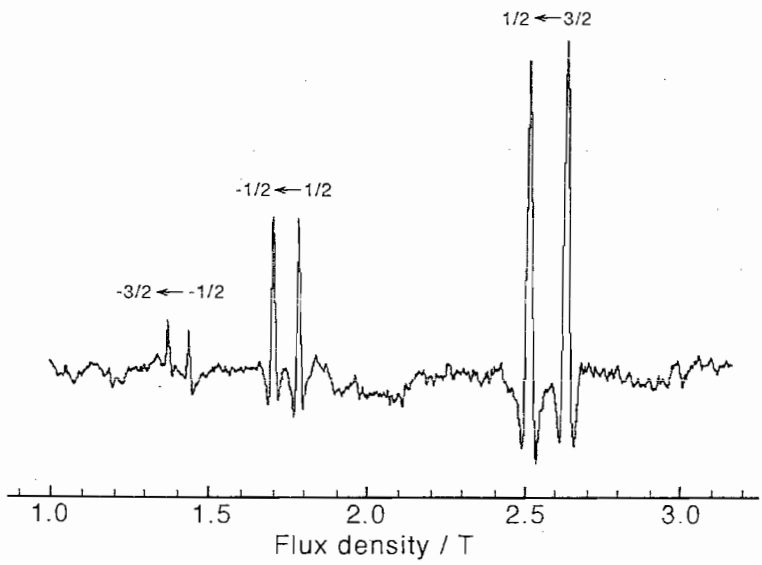

Fig. 2. Part of the mid-infrared LMR spectrum of the CD radical, recorded using the Faraday rotation technique so that the signals appear as first derivatives of the dispersion line-shape. The CO laser line is $P(16)_{4,3}$ at 2000.09 cm^{-1}. The rotational transition is $N = 1 \leftarrow 2$, $J = 1\frac{1}{2}$ of CD in the (1,0) band. The obvious doubling arises from lambda-type doubling and the numbers above each pair of resonances give the M_J levels involved.

been changed slightly, the earlier value corresponding to $(g_L - g_r)$ or 1.000851 in the present work. In addition to the zero-point values, the vibrational dependencies of several parameters have been obtained. Deuteron hyperfine splittings were observed in the far-infrared spectra for the levels $v = 1$ and 2 which showed that the vibrational dependence of the four hyperfine parameters is insignificantly small. This implies that the electron distribution at the proton in the valence π orbital of CH is only weakly dependent on the bond length r, a rather unexpected result.

The parameter values given in Table 6 can be used to determine the equilibrium values by use of Eq. (1). The equilibrium values for the major parameters obtained in this way are given in Table 7. These values are significantly more reliable than those published earlier by Morino et al. [9], partly because the present measurements are intrinsically more accurate and partly because we have been able to include observations on the (3,2) band. The latter primarily explains why the previously determined vibrational parameters ($\omega_e = 2100.3457$ (10) and $\omega_e x_e = 34.15582$ (39) cm^{-1}) differ so much from the values given in Table 7. It is also possible to estimate the equilibrium values by isotopic scaling of the corresponding values for CH [12,19,20]. The values obtained are also given in Table 7 and agree very well with the directly determined values (particularly for the vibrational and rotational parameters), confirming the correctness of our general procedure. The small differences between these two sets of values arise primarily from a breakdown of the Born–Oppenheimer approximation [21]. In Table 7, we also give the value for the equilibrium bond length r_e calculated from the value for B_e; once again, there is a small difference with the corresponding value for CH. As Morino et al. [9] point out, there are small non-adiabatic corrections to the value for B_e (and to the other parameters) which have to be taken into account if the correct Born–Oppenheimer value for the equilibrium bond length is to be obtained. We hope to explore these effects in a future paper.

One particularly interesting parameter determined in the present analysis of the CD data is α_{g_L} which gives the vibrational dependence of the orbital g-factor. The quality of fit was significantly improved by the inclusion of this parameter. In general, the major Zeeman parameters are expected to be independent of the vibrational quantum number since they are purely electronic properties of the molecule. This weak dependence of the orbital g-factor may arise from the spin–orbit mixing between the $X^2\Pi$ state of CD and the low-lying a $^4\Sigma^-$

Table 6
Molecular parameters for CD in the $X^2\Pi$ state determined from the analysis of available spectra

Parameter	Value (MHz)	Value (cm^{-1})
ν_0	60 918 834.9 (53)[a]	2032.03360 (18)[a]
$\omega_e x_e$	1 041 115 (17)	34.72785 (58)
$\omega_e y_e$	4241.1 (30)	0.14147 (10)
$\omega_e z_e$	−0.1343[b]	−0.004481[b]
A_0	842 308.59 (30)	28.096390 (10)
α_A	4361.3 (26)	0.14548 (87)
β_A	−43.8 (87)	$-0.146\ (29) \times 10^{-2}$
γ_0	−423.797 (75)	−0.0141363 (25)
α_γ	18.30 (22)	$0.6104\ (74) \times 10^{-3}$
B_0	230 896.080 (42)	7.7018642 (14)
α_B	−6362.79 (32)	−0.212240 (11)
β_B	$21.345\ (96) \times 10^{-2}$	$0.7120\ (32) \times 10^{-3}$
D_0	12.8216 (12)	$0.427683\ (41) \times 10^{-3}$
α_D	−0.1148 (40)	$-0.383\ (13) \times 10^{-5}$
β_D	-0.74×10^{-2b}	-0.27×10^{-6b}
H_0	0.4751×10^{-3b}	0.1585×10^{-7b}
p_0	544.41 (19)	0.0181597 (62)
α_p	−17.55 (31)	$-0.585\ (10) \times 10^{-3}$
p_D	$-0.47\ (13) \times 10^{-1}$	$-0.158\ (43) \times 10^{-5}$
q_0	339.455 (59)	0.0113230 (20)
α_q	−9.502 (215)	$-0.3170\ (72) \times 10^{-3}$
q_D	$-0.761\ (23) \times 10^{-1}$	$-0.2540\ (77) \times 10^{-5}$
α_D	$0.193\ (77) \times 10^{-1}$	$0.65\ (26) \times 10^{-6}$
a	8.05 (33)	$0.268\ (11) \times 10^{-3}$
b_F	−8.99 (29)	$-0.2999\ (95) \times 10^{-3}$
c	8.90 (55)	$0.297\ (18) \times 10^{-3}$
d	7.06 (30)	$0.235\ (10) \times 10^{-3}$
g_S	2.0020[b]	
g_L	0.999296 (74)	
α_{g_L}	$-0.422\ (79) \times 10^{-3}$	
g_l	$0.1313\ (37) \times 10^{-2}$	
g_r	$-0.1555\ (13) \times 10^{-2}$	
g_l'	0.1178×10^{-2b}	
g_r'	-0.1470×10^{-2b}	
g_N	0.857438[b]	

[a] Numbers in parentheses are one standard deviation of the least-squares fit, in units of the last quoted decimal place.
[b] Parameter constrained to this value in the fit (see text).

Table 7
Equilibrium values of molecular parameters for CD in the $X^2\Pi$ state

Parameter[a]	Value (present work)	Value (scaled from CH)[b]
ω_e	2101.05193 (55)[a]	2100.4495
$\omega_e x_e$	34.72785 (58)	34.7387
$\omega_e y_e$	0.14147 (10)	0.1439
B_e	7.8079823 (55)	7.795193
α_B	−0.212240 (11)	−0.212385
β_B	$0.7120\ (32) \times 10^{-3}$	0.9678×10^{-3}
D_e	$0.427683\ (41) \times 10^{-3}$	0.428246×10^{-3}
α_D	$-0.383\ (13) \times 10^{-5}$	-0.5518×10^{-5}
A_e	28.02402 (44)	28.05212
α_A	0.14548 (87)	0.13906 (87)
γ_e	−0.0144415 (45)	−0.014011
α_γ	$0.6104(74) \times 10^{-3}$	
g_l	$0.1313\ (37) \times 10^{-2}$	0.1275×10^{-2}
g_r	$-0.1555\ (13) \times 10^{-2}$	-0.1520×10^{-2}
r_e	1.11887138 (35)	1.119788

[a] Values given in cm^{-1} except for bond lengths which are in Å and g-factors which are dimensionless.
[b] Value calculated by isotopic scaling of the corresponding value for CH in its $X^2\Pi$ state [12,19,20]. The ratio of the reduced masses $\mu(CD)/\mu(CH)$ is 1.854964875.

Table 8
Calculated vibrational transition probabilities for CD in the $X^2\Pi$ state

Vibrational transition	Transition probability (a.u.)[a]
(1,0)	2.326×10^3
(2,1)	5.097×10^3
(3,2)	7.032×10^3
(4,3)	7.452×10^3
(5,4)	9.622×10^3

[a] The vibrational transition probability is equal to the square of the transition moment $\langle v'|\mu|v\rangle$. 1 a.u. $\approx$ (2.54 Debye)^2.

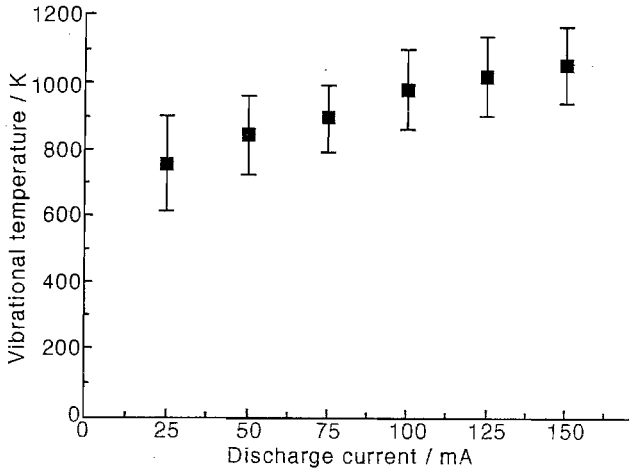

Fig. 3. The vibrational temperature of CD in the electric discharge used in the mid-infrared experiments, plotted as a function of the electric current.

state which lies some 6000 cm^{-1} above it. Such effects are known to be detectable in accurate Zeeman measurements as shown, for example, by Brown et al. [22].

The CD radical was produced in an electric discharge in the mid-infrared LMR experiments. It is possible to measure the vibrational temperature of the molecular sample under these conditions provided that the transition probabilities are known. We have calculated these probabilities from the RKR potential for CD in its $X^2\Pi$ state [19], using the electric dipole moment function given by Hettema and Yarkony [23]. The resultant vibrational transition probabilities are given in Table 8. Dividing the observed signal intensities for comparable transitions in the different vibrational bands by the transition probabilities allows the vibrational temperature to be determined. The population distribution followed Boltzmann behavior closely. The resultant dependence of the vibrational temperature on the discharge current is shown in Fig. 3. Extrapolation of these results confirmed that signals in the (4,3) band of CD would be too weak to be observable in our experiments.

Acknowledgments

We are very grateful to Dr. Steve Davidson for help with some of the measurements made in Boulder. We also thank Clare Nash who organised the data for the least-squares fit.

References

[1] J.E. Butler, J.W. Flemming, L.P. Goss, M.C. Lin, Chem. Phys. 56 (1981) 355–365.
[2] W.W. Duley, D.A. Williams, Interstellar Chemistry, Academic Press, London, 1984.
[3] O.E.H. Rydbeck, J. Elldér, W.M. Irvine, Nature 246 (1973) 466–468.
[4] G.J. Stacey, J.B. Lugten, W.M. Genzel, Astrophys. J. 313 (1987) 859–866.
[5] T. Shindei, Jpn. J .Phys. 11 (1936) 23–34.
[6] L. Gerö, Z. Phys. 118 (1941) 709–721.
[7] G. Herzberg, J.W.C. Johns, Astrophys. J. 158 (1969) 399–418.
[8] J.M. Brown, K.M. Evenson, J. Mol. Spectrosc. 136 (1989) 68–85.
[9] I. Morino, K. Matsumura, K. Kawaguchi, J. Mol. Spectrosc. 174 (1995) 123–131.
[10] T.J. Sears, P.R. Bunker, A.R.W. McKellar, K.M. Evenson, D.A. Jennings, J.M. Brown, J. Chem. Phys. 77 (1982) 5348–5362.
[11] A. Hinz, D. Zeitz, W. Bohle, W. Urban, Appl. Phys. B 36 (1985) 1–4.
[12] J.M. Brown, K.M. Evenson, J. Mol. Spectrosc. 98 (1983) 392–405.
[13] P.F. Bernath, J. Chem. Phys. 86 (1987) 4838–4842.
[14] J.M. Brown, E.A. Colbourn, J.K.G. Watson, F.D. Wayne, J. Mol. Spectrosc. 74 (1983) 294–318.
[15] J.M. Brown, M. Kaise, C.M.L. Kerr, D.J. Milton, Mol. Phys. 36 (1978) 553–583.
[16] J.M. Brown, J.K.G. Watson, J. Mol. Spectrosc. 65 (1977) 65–74.
[17] J.P. Towle, J.M. Brown, Mol. Phys. 78 (1993) 249–261.
[18] G. Herzberg, Spectra of Diatomic Molecules, Van Nostrand, Princeton, NJ, 1950.
[19] P.F. Bernath, C.R. Brazier, T. Olsen, R. Hailey, W.T.M.L. Fernando, C. Woods, J.L. Hardwick, J. Mol. Spectrosc. 147 (1991) 16–26.
[20] C.R. Brazier, J.M. Brown, Can. J. Phys. 62 (1984) 1563–1578.
[21] J.K.G. Watson, J. Mol. Spectrosc. 80 (1980) 411–421.
[22] J.M. Brown, C.R. Byfleet, B.J. Howard, D.K. Russell, Mol. Phys. 23 (1972) 457–468.
[23] H. Hettema, D.R. Yarkony, J. Chem. Phys. 100 (1994) 8991–8998.